

# Using WISE data to study the stellar populations of giant and dwarf ellipticals

Martijn de Vries

November 24, 2012

## Abstract

This work investigates the Color-Magnitude (C-M) relation for early-type galaxies. The recent WISE and Spitzer infrared surveys have opened up the possibility to study the C-M relation for galaxies in the near- and mid-Infrared. For the C-M relation four different samples from different sources are used, ranging from a Virgo Cluster sample of dwarf ellipticals to a large sample of bright early-types from the Sloan Sky Survey. The WISE survey is used to determine the [3.4]-[4.6] and [4.6]-[12] colors of all the samples, corresponding with the observational bands of the WISE mission. These infrared colors give us information about the possible presence of Asymptotic Giant Branch (AGB) stars in the early-type dwarfs, and the age and metallicity gradient of the galaxies. Although the results for the fainter galaxies are noisy, we find a clear C-M relation indicative of a metallicity gradient. The outlier galaxies, in both the [3.4]-[4.6] and [4.6]-[12] colors, are then age deviations from the main C-M relation, which is strong evidence that AGB stars are present in these galaxies.

For the larger early-types we find a nearly flat slope, meaning that there is no real metallicity dependency for those galaxies. In this sample we also find outliers, but many of these can also be attributed to Active Galactic Nuclei (AGN's) which are more commonly present in larger elliptical galaxies. The sample from the Sloan Sky Survey is harder to fit into the C-M relation, mainly due to redshift effects, further amplified by the reddening effects of the CO absorption band. However, selecting a subsample with lower redshift does flatten the slope, causing it to closer agree with the other sample of similar type galaxies.

# 1 Introduction

This work will take a look at the Color-magnitude (C-M) diagrams of dwarf elliptical galaxies in several infrared colors. C-M diagrams have been used since the 1970s to study the stellar populations of galaxies, mostly in the optical (Sandage, 1972). Here we extend these studies to the mid-IR, which is being opened up to us by the satellites Spitzer and WISE (Wide-field Infrared Survey Explorer).

It has been known for a few decades now that early-type (elliptical) galaxies show a tight C-M relation in several bands, such as U-B (Sandage, 1972). A color-magnitude relation allows us to derive some properties of the stellar populations. The fact that this relation is so tight makes it possible to derive some information about the stellar populations of galaxies, provided that a few basic assumptions are made: 1) The C-M relation joins the galaxies that at each magnitude are the oldest (Peletier 2012); 2) Along the C-M relation the metallicity decreases (i.e., larger systems have a higher metallicity) (Peletier 2012). So, by projecting the galaxies onto the C-M relation one can find the metallicity from the magnitude, and the relative age from the distance to the C-M relation. Trying to separate the influence of metallicity and influence of age is a problem known as the age-metallicity degeneracy (Peletier 2012). With only colors it is virtually impossible to break this degeneracy.

Especially in the infrared, the integrated color of early-type galaxies is strongly influenced by Asymptotic Giant Branch (AGB) stars. AGB stars are believed to be the main sources of dust creation in the universe, and because heated dust emits in the infrared, it can have a considerable reddening effect on the color of a dwarf galaxy (Draine, 2009).

The presence of AGB stars in a galaxy gives us more insight in the evolution and history of the galaxy. Because AGB stars are low-to-medium mass stars that have evolved off the stellar main branch, they are an indication of the age of a system. Galaxies with AGB stars must have undergone star formation 1-2 Gyr ago, while an early-type galaxy that has no AGB stars at all indicates that all star formation has happened long ago and that the galaxies are even older. Here in this work our aim is to study the contribution of AGB stars in galaxies. Since they have a strong contribution in the mid-IR, we study C-M relations there. AGB stars are the reason we can make the assumptions about the C-M relation as stated above: because AGB stars are an indicator of age and have a considerable reddening effect on early-type dwarfs, we make the assumption that metallicity varies along the main relation, and that deviations from this relation say something about the age of the galaxy (Peletier et al., 2012).

In this work we will be studying a number of samples that contain different kind of galaxies: dwarf ellipticals and irregulars (dE's and dIrr's) and giant ellipticals. A review of the use of dwarf Ellipticals is provided by Lisker et al.,

(2012). In this article it is explained that dE's can be a useful indication of the evolutionary history of an environment, because their number density depends strongly on galaxy density and because they are easily destroyed by gravitational encounters.

The data we used comes from the WISE survey. WISE is a NASA mission that mapped the entire sky in the infrared throughout 2010 (Wright et al., 2010). The thermal emission of the earth interferes heavily with ground-based infrared observations, which is why colors in the mid-IR region have only recently opened up for more extensive study. The WISE mission was the first all-sky infrared survey since IRAS in 1983, with a sensitivity of around twenty times higher ,thanks to advances in technology (Brown, 2009).

The WISE survey has four different observational bands at 3.4, 4.6, 12 and 22 microns respectively. Here we will be using two different colors: the [3.4]-[4.6] color and the [4.6]-[12] color. Because infrared surveys are rare, these kind of colors have not been well-researched yet. In section 2 we will go into more detail about the interpretation of these colors.

For each observational band, the survey uses eight different radii. They are shown in Table 1 (W1=[3.4], W2 = [4.6], etc.):

| bands      | 1     | 2     | 3     | 4     | 5     | 6     | 7     | 8     | units  |
|------------|-------|-------|-------|-------|-------|-------|-------|-------|--------|
| W1, W2, W3 | 5.50  | 8.25  | 11.00 | 13.75 | 16.50 | 19.25 | 22.00 | 24.75 | arcsec |
| W4         | 11.00 | 16.50 | 22.00 | 27.50 | 33.00 | 38.50 | 44.00 | 49.50 | arcsec |

Table 1: WISE survey radii for the different bands

## 2 Color Interpretation

As mentioned above, the [3.4]-[4.6] and [4.6]-[12] colors are not well-researched, but the SAURON project paper (number XX, Peletier et al., 2012) gives some excellent interpretations for the similar [3.6]-[4.5] color, from the Spitzer IRAC observations. A comparison between the Spitzer and WISE colors is made in section 3.3.

The luminous spectrum of a galaxy is not homogeneous: the inner part of a galaxy can be bluer or redder than the outer part, depending on the galaxy and the range of the spectrum that is studied. This change in color as a function of the radius of the system is called a color gradient.

In the SAURON paper, it is explained that elliptical galaxies tend to become bluer with bigger aperture (i.e. a negative gradient) in most parts of the op-

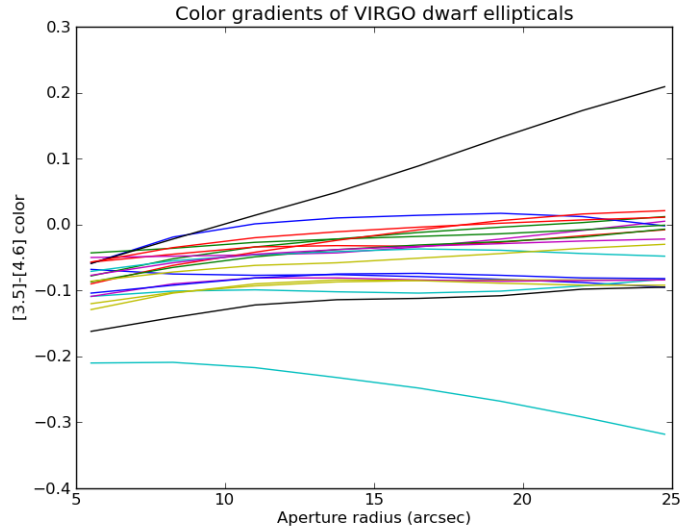


Figure 1: Color gradients of a random sample of dwarf Ellipticals in the Virgo Cluster. Most of the color gradients are positive.

tical spectrum (Peletier et al., 1990). But in this part of the infrared they do not always. Fig 1 shows some [3.4]-[4.6] color gradients plotted from the Virgo cluster elliptical galaxies. The profile is generally quite flat, but on average the color reddens slightly (i.e. positive gradient) with increasing aperture.

The reddening of galaxies with increasing aperture can be explained by the CO absorption band. This band blocks a lot of light in the 4.6 micron range. Because the metallicity gradient in ellipticals is generally negative, the CO-band becomes less deep going outward, and the [4.6] band becomes more important relative to the [3.4] band. Even though the temperature also increases with lower metallicity, causing the light to be bluer, the effect from the lowering of the CO absorption band is stronger (Peletier et al., 2012) and the color will become redder (Fig. 2) (Peletier et al., 2012).

The paper also notes that the main source of emission in the Near-Infrared (NIR) is from stellar light. The contribution of stellar light decreases as we go further into the infrared and other factors start to contribute more. An important factor going further into the infrared is dust emission. This dust is linked to the presence of AGB stars, as described in the introduction.

Another important feature, described in Shapiro et al. (2010) is an emission feature at about 8 micron. This feature comes from PAH transitions excited by young stars, and is therefore indicative of star formation. We thus have have

M giants,  $\log(g)=0.0$ , solar Z, solar mass

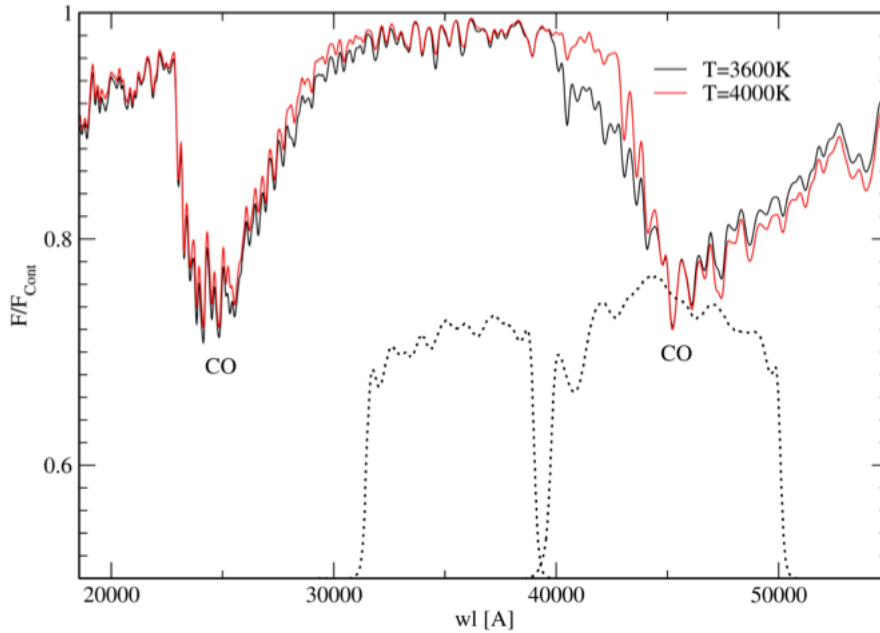


Figure 2: “Spectral energy distributions of two M-type giant stars from the MARCS library (Bressan, private communication). Two CO molecular absorption bands are visible, the second one of which falls in the 4.5 $\mu$ m filter of IRAC while the 3.6 $\mu$ m filter is free from molecular bands. The figure shows that the absorption feature is stronger for cooler stars and therefore that older stars have bluer [3.6]-[4.5] colors. The IRAC passbands are indicated in dashed lines.” Graph and description from Peletier et al., 2012.

two possible causes for strong colors further into the infrared: either the color is caused by warm dust from AGBs (older populations), or it is indicative of star formation and therefore a younger population. The [3.4]-[4.6] color is a purely stellar color, affected by AGB stars. The [4.6]-[12] color depends strongly on the dust/PAH content. Connecting the 2 colors gives important information about whether both causes are related.

## 3 Data Analysis

### 3.1 The samples

For the galaxy color-magnitude diagram, we chose to incorporate a number of samples of different sizes and magnitudes, so that the range in luminosity of the data is bigger resulting in more meaningful information. The final C-M diagram is comprised of four different samples with different galaxy properties. To compare them properly we look at the different properties of these samples one by one in the next four paragraphs.

#### 1) The SMAKCED sample

This sample was originally used by the SMAKCED project (see Janz et al., 2012). 'SMAKCED' stands for 'Stellar population properties, Masses and Kinematics for the large representative sample of Cluster Early-type Dwarfs'. The SMAKCED project uses this sample to investigate different properties of dwarf ellipticals and lenticulars. The sample consists of 168 galaxies from the Virgo Cluster Catalog (VCC) (Binggeli et al., 1985). The galaxies are all relatively small and have luminosity range  $-16 \leq M_r \leq -19$  (Janz et al., 2012).

#### 2) The SAURON sample

This sample is taken from the SAURON project paper II (de Zeeuw et al. 2002). The sample consists of 72 galaxies total in the E, S0 and Sa groups, with 24 galaxies in each group. Because we cover early-type galaxies, we did not include the Sa galaxies. This leaves us with a sample of 48 galaxies to use. These galaxies have a higher luminosity than those of the SMAKCED sample, with magnitudes ranging from about  $-26 \leq M_{[3.4]} \leq -22$ . They are useful to see how the C-M diagram continues into the higher-mass range.

#### 3) The MAGPOP sample

The MAGPOP project investigates the star formation history of dwarf galaxies. To do this, they have selected a few different samples. Apart from the sample of dE's (Toloba et al., 2011) this survey also contains a sample of star forming dwarfs. We have used a sample of 61 dwarf galaxies. The sample has  $m_B < 15.5$ , the galaxies are part of the VCC (Binggeli et al., 1985), and are all of type S (spiral) or Im (irregular).

#### 4) The SDSS sample

This sample consists of observations made by the Sloan Digital Sky Survey (SDSS). The sample was selected in a paper by Bernardi and consists of a total of 8666 galaxies (Bernardi et al., 2003). The galaxies have redshifts  $0.01 < z < 0.3$  and numerous other selection criteria that can be found in that paper. The galaxies are early-type but not dwarfs, which means the luminosities will be higher than in the SMAKCED sample, of comparable magnitude to the SAURON sample, ranging from  $-28 \leq M_{[3.4]} \leq -24$ .

### 3.2 Processing the sample data

To retrieve the [3.4]-[4.6] and [4.6]-[12] colors, we needed to get the WISE survey data, available on the NASA Infrared Science Archive (IRSA). The survey does not always manage to find all of the target sources, depending on the cone search radius: if the search radius is too big it sometimes finds multiple sources corresponding to the given coordinates. For every table entry, a parameter is provided showing the radial distance between the precise set of coordinates and the coordinates where WISE sees a source. If two or more sources are found for a coordinate set, the one with the lowest radial distance is chosen. Sometimes no source at all is found within the search radius of the given coordinates. Because of this, some data points of the samples were 'lost' during the multi-object search. For the first three samples, the missing data points were manually added, since there were only a few. Because the SDSS sample has so many data points, the data loss was negligible. This means that for the SDSS sample we used 8619 data points out of the original 8666.

An aperture of 5.5 arcsec radius of a nearby, big elliptical galaxy will only manage to capture some inner part of the galaxy, while the same photograph for a far-away dwarf galaxy will capture the entire galaxy. Because of the color gradient (see section 2) this will lead to skewed results.

Therefore, the notion of an effective radius is useful: an effective radius  $R_e$  is defined as the radius inside which half of the total emitted light of the galaxy is emitted. This parameter gives a quantitative way of comparing the galaxy colors within a certain radius. For the C-M diagram we used  $R_e/8$ . The reason why we chose  $R_e/8$  rather than  $R_e$  is because most of the galaxies in the SAURON sample have such a big effective radius that the biggest WISE aperture would not be able to capture it.

Because the SMAKCED sample consists of dwarf galaxies, we simply used the lowest aperture (5.5 arcsec) for  $R_e/8$ , since  $R_e/8$  is always smaller. An attempt to extrapolate inwards was made, but this leads to incorrect data. The absolute magnitude was obtained by using the WISE band 1 apparent magnitude and applying the distance modulus of the Virgo cluster, which was found in literature to be 31.04 (Blakeslee, 2009).

For the SAURON sample the effective radii are given in the SAURON paper XIX (Falc3n-Barroso et al., 2011). This paper also lists the absolute magnitudes for the sample, which were used to plot. The Spitzer [3.6] magnitude will differ slightly from the WISE [3.4] magnitude, but this difference is negligible. The colors were interpolated and calculated at  $R_e/8$ , also taken from this paper.

For the MAGPOP sample the same applies as for the SMAKCED sample: these are dwarf galaxies and therefore we used the lowest WISE aperture to calculate the colors with. For the magnitudes, the Virgo distance modulus was also used.

For the SDSS sample the lowest aperture was also used. This is because these are galaxies with high redshift, therefore they are far away and the 5.5 arcsec aperture will be bigger than  $R_e/8$ . The magnitudes were calculated in a slightly different way. The paper that analyses the sample lists absolute magnitudes, but those are in optical bands and therefore differ significantly from the infrared magnitude.

We determined the way these colors relate. In literature we find that  $r^* = V - 0.49(B-V) + 0.11$  (Fukugita et al.,1996). The B-V color for ellipticals is around 1, we then get  $r^* = V - 0.38$ . From the SAURON XIX paper we obtain  $V = [3.6] + 3.2$ , with a readability uncertainty of 10%, so we get  $r^* = [3.6] + (3.2 \pm 0.32) - 0.38 = [3.6] + 2.86 \pm 0.32$  (Falc3n-Barroso et al., 2011). We can now use the SDSS tabulated  $r^*$  colors and convert them into  $[3.6]$  magnitudes.

For this sample, different redshift selections were also made. Because the SDSS sample galaxies all have a relatively high redshifts ranging from 0.01 to 0.3, there is a reddening effect and galaxies with higher redshift will have a redder color. The reddening is made even stronger by the fact that the CO absorption band in the 4.6 micron filter gets shifted out of the filter, which gives a sudden jump increase in the colors. It is therefore useful to make some redshift selections for this sample. Different redshift plots are shown below. Once all the data for the different samples is collected, the color-magnitude diagram can be plotted.

### 3.3 Color difference between Spitzer and WISE

Because we use sample data from the Spitzer telescope, it is useful to see how the colors measured with Spitzer and WISE compare. Therefore we have compared the colors for the SAURON sample as measured by Spitzer and WISE. The Spitzer data was provided by Peletier, 2012. The WISE data was obtained as described above, and then interpolated to obtain the color at the correct radius. Since we are using the Spitzer data at  $R_e/8$ , we did the comparison at this radius. The result is plotted in Figure 3.

The comparison will lead to some galaxies with relatively high color differences: as mentioned above, we can only interpolate and not extrapolate, as this will lead to incorrect values. Therefore, for every  $R_e/8$  lower than WISE's minimum aperture radius of 5.5 arcsec, we simply used the color at 5.5 arcsec. From the limited data points it also seems that the color difference increases a bit with bigger radius. A large part of the sample has  $R_e/8$  below 5.5, and a lot of scatter is visible there. This scatter probably comes from the fact that while the galaxies have  $R_e/8$  below 5.5 arcsec, the color is measured at 5.5 arcsec.

Overall we found an average color difference of -0.018 with a standard deviation

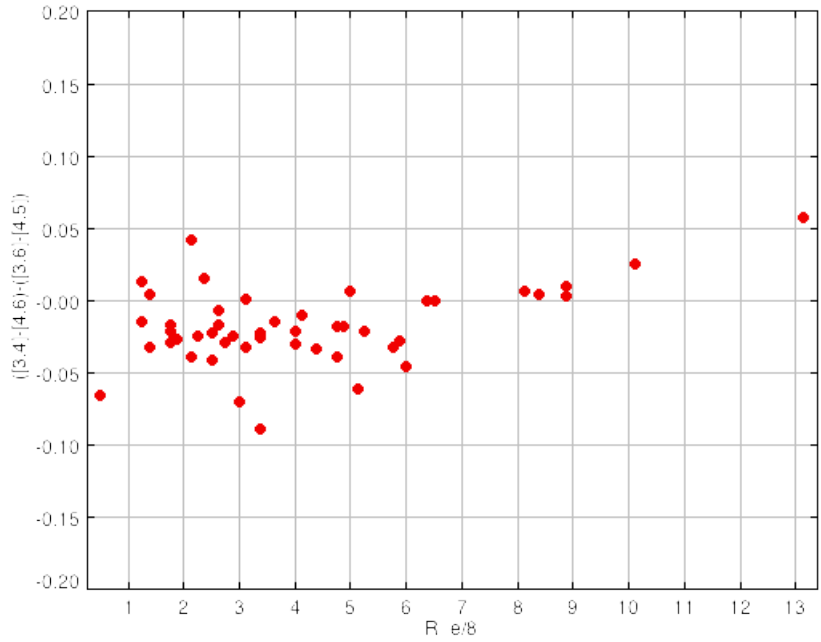


Figure 3: Difference between the Spitzer and WISE colors for the SAURON sample.

of 0.027, which compared to the overall errors in the SAURON sample is not big enough to correct for.

## 4 Results

To show the results as clearly as possible, we will first show the C-M diagram for the SAURON sample individually, and the SMAKCED and MAGPOP samples together, including the error bars for [3.4]-[4.6]. The errors are obtained from WISE at the 5.5 arcsec aperture radius.

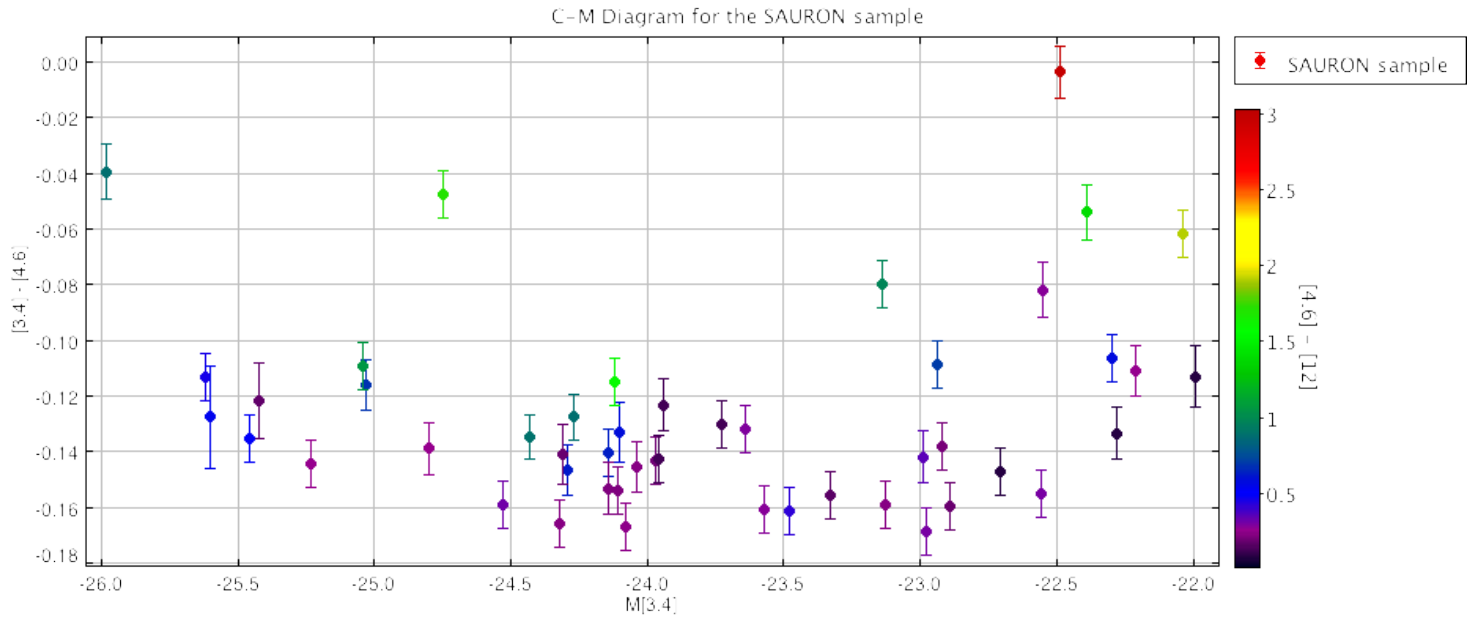


Figure 4: The C-M diagram for the SAURON sample with errors for [3.4]-[4.6].

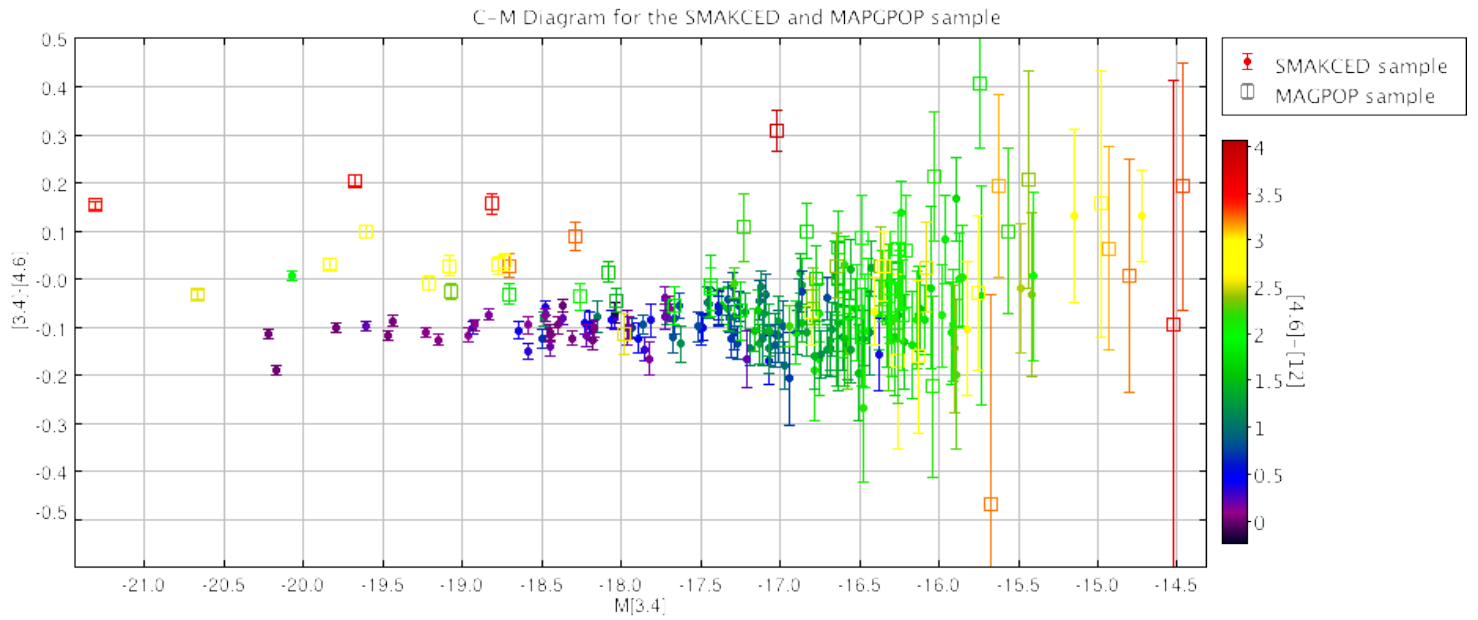


Figure 5: The C-M diagram for the MAGPOP and SMAKCED sample with errors for [3.4]-[4.6]. Circles are SMAKCED data points, squares are MAGPOP data points.

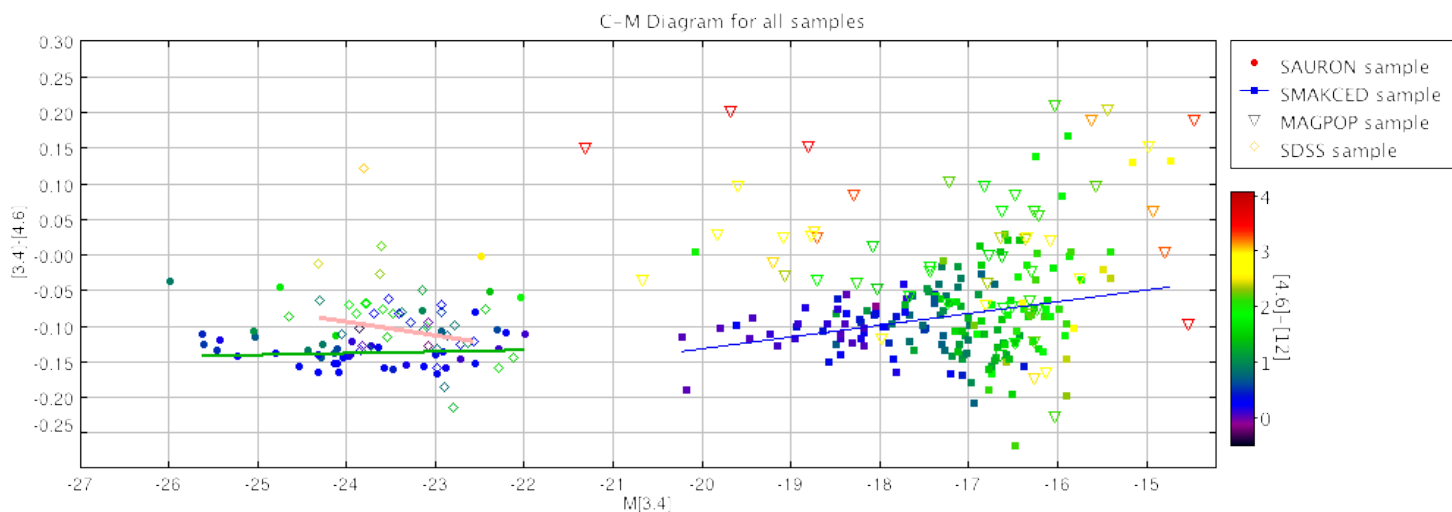


Figure 6: *C-M diagram with  $z < 0.03$  for the SDSS sample. The symbols indicate the sample. The color of the symbols is given by the  $[4.6]-[12]$  color of the plotted galaxy.*

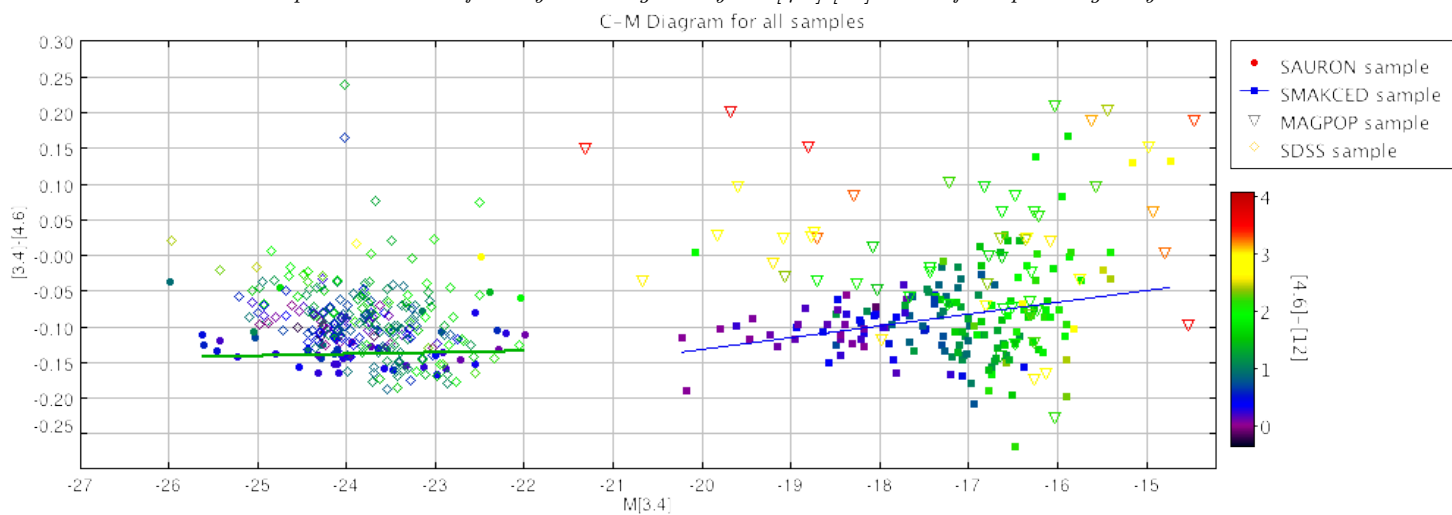


Figure 7: *C-M diagram with  $0.03 < z < 0.05$  for the SDSS sample. The symbols indicate the sample. The color of the symbols is given by the  $[4.6]-[12]$  color of the plotted galaxy.*

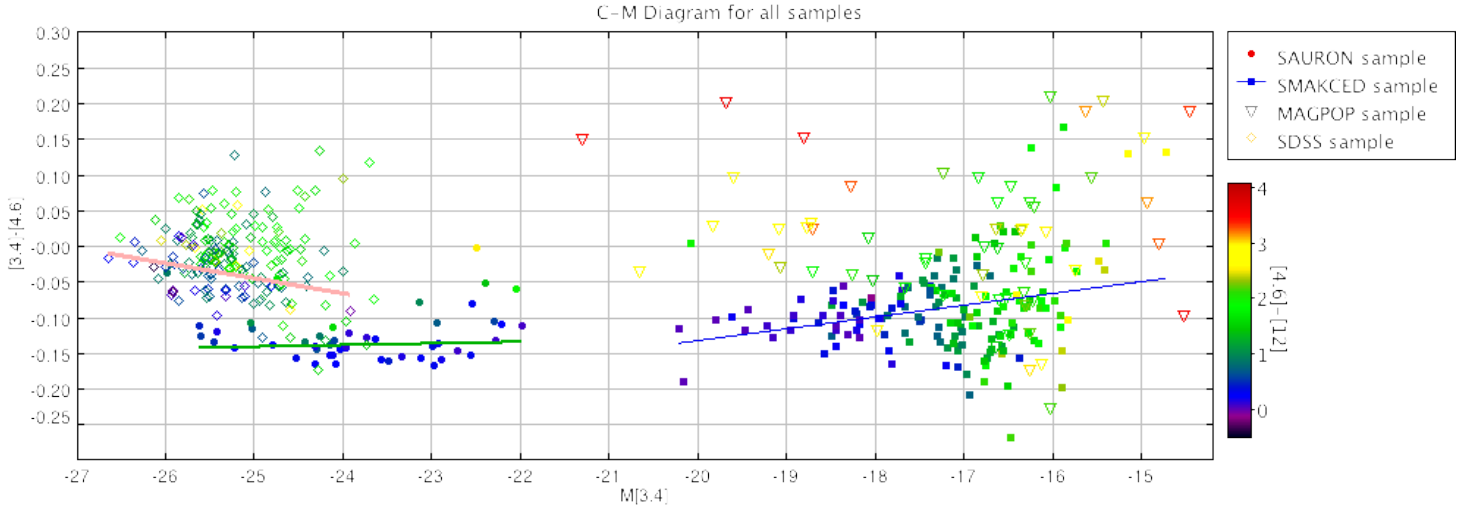


Figure 8: C-M diagram with  $z < 0.1$  and  $S/N \geq 7$  for the SDSS sample. The symbols indicate the sample. The color of the symbols is given by the  $[4.6]-[12]$  color of the plotted galaxy.

Several features can be seen in the figures. First, there is a noticeable positive slope in the SMAKCED sample. This is the main  $[3.4]-[4.6]$  metallicity relation: for fainter galaxies the metallicity seems to increase. Along this relation, the  $[4.6]-[12]$  color stays the same, between zero and one below a Mag of -18, results get very noisy. There are numerous galaxies that deviate from the  $[3.4]-[4.6]$  mag relations and also show red  $[4.6]-[12]$  colors. Although the result for the faintest dwarfs are noisy, it shows that younger objects, as measured from the C-M-relation, show dust emission, which is probably dust around AGB stars. The fact that the galaxies have high colors in both  $[3.4]-[4.6]$  and  $[4.6]-[12]$  links AGB presence and star formation, and is a clear indication that the galaxies deviating from the C-M relation are indeed younger objects.

A peculiar outlier in the SMAKCED is VCC 758 (or NGC 4370). This galaxy at mag -20.1 has uncharacteristically high colors in both  $[3.4]-[4.6]$  and  $[4.6]-[12]$  compared to other galaxies around this magnitude. This can be explained by the fact that VCC 758 is in many ways closer to a spiral galaxy and is likely to have a lot more dust and therefore redder colors than the other galaxies of the SMAKCED sample.

Another cause of the red colors could be AGN. The radiation from AGN causes the color to redden in the infrared (Polletta et al., 2006). However the presence of AGN is unlikely in early-type dwarfs. In the SAURON sample there are some galaxies that are known to have an AGN, such as NGC 2974 and NGC 4486. These are both outliers with high  $[3.4]-[4.6]$  and  $[4.6]-[12]$  colors. This means

that to give a full description the galaxies in this sample we would have to look at the galaxies case-by-case.

The slope of the SMAKCED sample can be extended to the SAURON sample of bigger galaxies. The SAURON sample has some quiescent galaxies with low [3.4]-[4.6] and [4.6]-[12] colors. These have a slope that is nearly flat. Above this line are some galaxies that have higher colors, which can again be attributed to the presence of AGB stars. The fact that the slope is flat, indicates that for the SAURON sample there is low dependence on metallicity, and no noticeable age dependency, since the vertical deviations indicating the presence of AGB stars happen along the entire relation.

For the SDSS sample, its interesting to look what happens at the different redshifts. Weve made several different redshift selections: the galaxies with redshift  $0.01 < z < 0.03$ , a second plot with  $0.03 < z < 0.05$ , and a final one for  $z \geq 0.1$  and  $S/N \geq 7$  We can see straight away that the last one, for  $z \geq 0.1$  and  $S/N \geq 7$ , is difficult to use. The effects of reddening are strong and clearly visible. For this band the K-correction is large, because the CO-band at 4.5 micron shifts out of the [4.6] band.

The slope of the SDSS sample is somewhat surprising, especially when comparing it to the other samples. What we expect to see is that is either flat or slightly positive, similar to the SAURON and SMAKCED samples: even ignoring the galaxies that are active in the [4.6]-[12] color and only use the galaxies with a [4.6]-[12] color below 1. This might be explained by a observational bias effect: at higher redshifts we only see galaxies with higher magnitudes, therefore the galaxies with higher magnitudes have a stronger redshift correction.

The fact that the slope is closer to being flat could indicate a flat slope, which would mean that for both the SDSS and SAURON samples, the [3.4]-[4.6] color depends less on metallicity than on age.

## 5 Conclusions

Our findings summarize as follows:

- In the near- and mid-IR a clear C-M relation is visible for early-type galaxies. For dwarf early-types, we see a slope indication a metallicity relation: fainter galaxies have higher metallicity. This relation flattens out for more luminous galaxies, meaning that for those galaxies there is no real metallicity dependence.
- Although the results for the fainter dwarfs are extremely noisy, outliers from the main C-M-relation are visible in both the [3.4]-[4.6] and [4.6]-[12] colors, linking the presence of Asymptotic Giant Branch stars (AGB stars) and star formation. This means that the vertical deviations from

the main C-M-relation are indicative of relative age, i.e., that these objects are younger than the objects on the main relation.

- For the bigger galaxies from the SAURON sample, the same deviancies are visible. However, some of the outliers are certainly attributable to Active Galactic Nuclei (AGN's), so this would have to be looked at on a case-by-case basis.
- The SDSS sample is difficult to fit into the C-M relation as a whole, because of the high redshift, further amplified by the CO-band reddening effects. This gives the main C-M relation of the SDSS sample a negative slope rather than a flat or positive one. It is however clearly visible that attempts to reduce the redshift effect (selecting only galaxies below certain redshift thresholds) flatten out the slope of this sample.

## Acknowledgements

First and foremost, thanks to my tutor, Reynier Peletier, whose expertise and passion for this subject have vastly improved this work. This work makes use of data products from the Wide-field Infrared Survey Explorer, which is a joint project of the University of California, Los Angeles, and the Jet Propulsion Laboratory/California Institute of Technology, funded by the National Aeronautics and Space Administration.

## References

Bernardi, M., Sheth R.K., Annis, J., Burles, S., Eisenstein D.J., Finkbeiner D.P., Hogg D.W., Lupton R.H., Schlegel D.J., SubbaRao M., Bahcall N.A., Blakeslee, J.P., Brinkmann J., Castander F.J., Connolly A.J., Csabai I., Doi M., Fukugita M., Frieman J., Heckman T., Hennessy G.S., Ivezi Z., Knapp G. R. Lamb D.Q., McKay T., Munn J.A., Nichol R., Okamura S., Schneider D.P., Thakar, A.R., York, D.G., 2003a AJ, 125, 1817

Binggeli B., Sandage A., Tammann G. A., 1985, AJ 90, 1681

Brown, Roz. "December 4th: The Wise Mission", 365 days of astronomy. 4 december 2009. Web. 14 october 2012 <http://365daysofastronomy.org/2009/12/04/december-4th-the-wise-mission/>

Draine B.T., 2009, ASP Conference Series 414, 453

Falcón-Barroso J., van de Ven G., Peletier R. F., Bureau M., Jeong H., Bacon R., Cappellari M., Davies R. L., de Zeeuw, P. T., Emsellem, E., Krajnovi D., Kuntschner H., McDermid, R. M., Sarzi, M., Shapiro, K. L., van den Bosch R. C. E., van der Wolk, G., Weijmans, A.; Yi, S., 201, MNRAS, 417, 1787

Fukugita M., Ichikawa T., Gunn J.E., Doi M., Shimasaku K., Schneider D. P., 1996, AJ, 111, 1748

Lisker T., Boselli A., den Brok M., Falcón-Barroso J., Hensler G., Janz J., Laurikainen E., Niemi S.-M., Peletier R.F., Salo H., Toloba E., 2012, ApJ, 745, L24

Mei S., Holden B.P., Blakeslee J.P., Ford H.C., Franx M., Homeier N.L., Illingworth G.D., Jee M.J., Overzier R., Postman M., Rosati P., Van der Wel A., Bartlett J.G., 2009 AJ, 690, 42

Peletier R.F., Cawson, M., Davies R.L., Davis, L.E., Illingworth G.D., 1990, ApJ, 100, 1091

Peletier R.F., Bacon R., Bureau M., Cappellari M., Davies R.L., de Zeeuw P.T., Emsellem E., Falcón-Barroso J., Kutdemir E., Krajnovi D., Kuntschner H., McDermid R.M., Sarzi M., Scott N., Shapiro K.L., van den Bosch, R.C.E., van der Wolk G., van de Ven, G., 2012, MNRAS, 419, 2031

Peletier R.F., 2012, "Stellar Populations": Proceedings of lectures given at the XXIIIrd Canary Islands Winter School; 71 pages; to appear in Secular Evolution of Galaxies, eds. J. Falcón-Barroso J. H. Knapen (Cambridge: Cambridge University Press), in press.

Sandage A., 1972, ApJ, 176, 21

Shapiro, K.L., Falcón-Barroso J., van de Ven G. , de Zeeuw P.T., Sarzi M., Bacon R., Bolatto A., Cappellari M., Croton D., Davies R.L., Emsellem E., Fakhouri O., Krajnovic D., Kuntschner H., McDermid R.M., Peletier R.F., van den Bosch R.C.E., van der Wolk G., 2009, MNRAS, 402, 2140

Toloba E., Boselli A., Peletier R. F., Gorgas J., 2011, EAS 48, 189

Wright E.L., Abid M., Benford D., Blain A., Cardon J.G., Cohen M., Cutry R.M., Duval V., Eisenhardt P.R.M., Fabinsky B., Gautier III T.N., Heinrichsen I., Howard J., Jarrett T., Kendall M., Kirkpatrick J.D., Larsen M., Leisawitz D., Liu F., Lonsdale C.J., McLean I., MC-Millan R.S., Mainzer A., Mather J.C., Mendez B., Naes L., Padgett D., Ressler M.E., Royer D., Schick S., Schwalm M., Shannon M., Skrutskie M., Stanford S.A., Tsai C.W., Walker R.G., Walsh A.L., 2010, AJ, 140, 1868